An Electrochemical System for the Study of Trans-Plasma Membrane Electron Transport in Whole Eukaryotic Cells

Journal:	*Analytical Chemistry*
Manuscript ID	ac-2017-048536.R1
Manuscript Type:	Article
Date Submitted by the Author:	11-Jan-2018
Complete List of Authors:	Sherman, Harry; University of Nottingham, Pharmacy Jovanovic, Carolyn; Boots UK Ltd Stolnik, Snow; University of Nottingham, Pharmacy Rawson, Frankie; University of Nottingham, School of Pharmacy

An Electrochemical System for the Study of Trans-Plasma Membrane Electron Transport in Whole Eukaryotic Cells

Harry G. Sherman[†], Carolyn Jovanovic[‡], Snow Stolnik[∞], Frankie J.Rawson[†]*

†Division of Regenerative Medicine and Cellular Therapies, School of Pharmacy, University of Nottingham, NG7 2RD, UK

∞Division of Molecular Therapeutics and Formulation, School of Pharmacy, University of Nottingham, NG7 2RD, UK

‡ Walgreens Boots Alliance, Nottingham, NG2 3AA, UK

ABSTRACT: The study of trans-plasma membrane electron transport (tPMET) in oncogenic systems is paramount to the further understanding of cancer biology. The current literature provides methodology to study these systems that hinges upon mitochondrial knockout genotypes, or the detection of ferrocyanide using colorimetric methods. However, when using an iron redox based system to probe tPMET there is yet to be a method that allows for the simultaneous quantification of iron redox states whilst providing an exceptional level of sensitivity. Developing a method to simultaneously analyze the redox state of a reporter molecule would give advantages in probing the underlying biology. Herein we present an electrochemical based method that allows for the quantification of both ferricyanide and ferrocyanide redox states to a highly sensitive degree. We have applied this system to a novel application of assessing oncogenic cell-driven iron reduction, and have shown that it can effectively quantitate and identify differences in iron reduction capability of three lung epithelial cell lines

All cells communicate with their environment via external electron transfer events. These events are mediated by (tPMETs) trans-plasma membrane electron transport systems. The development of new techniques to study cellular electron transfer via trans plasma membrane electron transport (tPMET) is required in order to shed light on its role in cellular homeostasis. The development of new assays for such purposes can yield new biological insight regarding their function. The output of the assays can then be applied for a number of broad applications, from the development of biosensors[1] and microbial fuel cells[2] through to identification of potential new targets for therapies in which tPMETs are thought to play a part, such as cancer[3].

tPMET plays a fundamental role within mammalian cells by facilitating the reduction of ferric iron at the duodenal brush broder[4], and detoxifying iron at the environment-exposed lung epithelium[5,6]. It is possible to probe these systems using redox mediators such as potassium ferricyanide (FIC)[7], but to date there has been no application of electrochemistry to simultaneously quantitate iron redox states in cancer biology. In this paper we provide an electrochemical based platform for studying tPMET through detection of multiple iron redox states to a highly sensitive degree, and by doing so we identify differences in the reductive capabilities of tPMET in three mammalian cancer cell lines.

Iron is an essential micronutrient for all forms of mammalian life[8,9,10,11]. Electron transfer across membranes is typically associated with respiratory electron transport within the mitochondria, but tPMET also plays a role within a multitude of processes[12] including pH control and signal transduction[13], apoptosis[14,15], antioxidation[16], and iron homeostasis[13,17,18].

The tPMET function of the non-transferrin bound iron transport system is evidenced to be mediated by a NAD(P)H:oxidoreductase system[18], ascorbate shuttle mechanism[19], or ascorbate or AFR-dependant transmembrane reductase system[19]. A widely accepted ferrireductase, duodenal cytochrome b_{561} (Dcytb), has been shown to be expressed in a wide variety of cell types including human erythrocytes[20], lung epithelium[21], K562 cells[22], astrocytes[23], and intestinal origin Caco-2 and HEP-G2 cells[24]. This is interesting as, apart from in the gut, 'free' non-transferrin bound iron (NTBI) is often undetectable, except in cases of iron overload[25,26]. tPMET systems may therefore be present as a protective measure if iron overload does occur, or be present at the plasma membrane of cells in different tissue throughout the body for a yet unknown functionality to those identified. This leads to a hypothesis that the role and upregulation of tPMET in cancer is to reoxidize cytosolic NADH to allow for continued glycolysis[3], in the case of the Warburg effect[27] occurring. Work has been carried out to look at the presence of tPMET in non-mitochondrial oxygen consumption, and it has been shown to have involvement not only in mitochondrial knockout (p^0) cells but also for oncogen-

ic cells that possess fully competent mitochondrial activity[28].

In light of tPMET mechanisms being present where there may be yet undiscovered functions, such as in the lung or within cancer metabolism in relation to NADH[3]. It is therefore imperative that we study tPMET in oncology to understand the underlying biochemistry, as this may lead to better diagnostic tools and therapeutics. Herein we described the development of a method that can be used to study tPMET by identifying different redox states of iron simultaneously. We then have used this method to identify and differentiate tPMET activity between cell types of the same tissue and origin – lung epithelium, as there has not been any comparison between cancerous cell lines tPMET activity in this manner.

The techniques used to study components of iron homeostasis[29] can include potentiometry, which has been used to assess redox properties of duodenal cytochrome b_{561}. Mackenzie et al[30] have used voltage-clamp experiments in elucidating how the divalent metal transporter 1 (DMT1) mediates both H^+-coupled Fe^{2+} transport in whole oocytes[31]. Others have used double electrochemical mediator systems to look at intracellular redox sites[32]. Baronian et al[33] have also used linear sweep voltammetry in the electroanalytical detection of catabolism in whole cell yeast. McDowall et al[34] have used amperometry to study the lysates of neuroblastoma cells, but do not investigate whole cell neuroblastoma cells and therefore they could not assess tPMET. Cancer tPMET (on intact cells) has been investigated by alternative methods to electrochemistry. Herst et al[3,35], Berridge et al[36] and Scarlett et al[37] have all used mitochondrial gene-knockout (ρ^0) cells as a way to study tPMET. Using HL60ρ0 cells they have demonstrated a link between tPMET and cell surface oxygen consumption, linked to the Warburg effect[27]. Avron and Shavit[38] previously developed a colorimetric assay to determine ferrocyanide (FOC) concentration, which could be used to study tPMET. This was improved upon by Lane et al[7], and used to study tPMET in a leukaemia cell line. These two colorimetric methods provide sound methodology to study tPMET at a high throughput level, but as they only quantitate for FOC they lack ability to quantify both iron redox states present. In the present work we develop an electrochemical assay capable of monitoring and quantifying the redox states of iron to provide new biological observation on the use of tPMETs in cancer cell lines.

We have developed an electrochemical assay using linear sweep voltammetry at a microelectrode, and in a first have subsequently applied this to study tPMET in cancer cells. We have developed a micromolar-level iron quantification method that is simple, with exceptionally low limits of detection, and that improves on current techniques to study tPMET on whole cells by allowing multiple redox state detection. This has led to new observations that cells from the same tissue behave differently in terms of how they use tPMET. This raises some interesting questions about the underlying biology and their function. This new application for electrochemistry has been fully validated with other analytical techniques which include biological toxicity assays and ICP-MS analysis of cellular iron content.

Experimental section

Materials. All reagents were purchased from Sigma-Aldrich, unless otherwise stated.

Characterisation of FIC/FOC redox states for calibration. 0.01 mM FIC and FOC (Acros Organics) solutions were both made in Hanks' Balanced Salt Solution (HBSS). The two solutions were mixed in a variety of combinations, from ratios 10:0 to 0:10 FIC:FOC to give concentrations (μM) of each redox state respectively at: 0:10, 1:9, 2:8, 3:7, 4:6, 5:5, 6:4, 7:3, 8:2, 9:1 and 0:10.

A three electrode system comprising a 33 μm carbon fibre working microdisk electrode, a saturated calomel reference electrode, and a platinum wire counter electrode was used (ALS Co. Ltd, Japan). An Autolab PGStat302A potentiostat with low current detection module (ECD) (Metrohm Autolab, Utrecht, Netherlands) and NOVA 2.1 software was used in all experiments.

Linear sweep voltammetry was performed with solutions containing differing ratios of oxidized and reduced forms of iron (as above) and were carried out by scanning from 500 mV to -150 mV, at a scan rate of 10 mV s^{-1}. A current range of 100 pA was used, with a low current module employed. A linear sweep voltammogram was recorded with the HBSS only acting as a control to allow for baseline subtraction. Between each solution tested the microelectrode was polished for 4 minutes using a PK-3 electrode polishing kit (ALS Co. Ltd, Japan). Pseudo-steady-state values were determined by assessing a first derivative function of the voltammogram and cross referencing with the original curve to clarify that this was the voltage the pseudo-steady state was located.

Stability of FIC in cell culture conditions. As outlined in **Method S-1** of Supplementary Information.

Investigation of electrode fouling. As outlined in **Method S-2** of the Supplementary Information.

Growth study. The three cell lines analyzed in this study were Calu-3, H1299 and A549 cells. All cell lines were originally purchased from ATCC. All cells were grown in DMEM (Dulbecco's Modified Eagles Medium) containing high glucose supplemented with 10% FBS (fetal bovine serum), 100 U/ml penicillin, 100 μg/ml Streptomycin and 24 mM HEPES (N-(2-Hydroxyethyl) piperazine-N′-(2-ethanesulfonic acid)) buffer. A549 cells were passage number 12 for the growth study, H1229 were passage number 13 and Calu-3 passage number 41. A549 and H1299 cells were seeded at 0.10 x 10^6 cells/well and Calu-3 cells at 0.25 x 10^6 cells/well in 12 well plates. Viability was tested each day for 10 days by first detaching cells from cell culture plates using 0.1 mL trypsin/EDTA, followed by addition of 10 μl cell suspension to 10 μl tryphan blue dye (TB). Dye exclusion analysis was then carried out using a Tecan microplate reader (Tecan Ltd, Weymouth, UK). A

growth curve was produced for each cell line, and a harvesting time selected that ensured all three cell lines were in an exponential growth phase when used in subsequent experiments. Calu-3 cells were hence harvested after a 4 days growth, and A549 and H1299 cells following 3 days growth. All cells were harvested at a confluency of ~90%.

Toxicity studies. The choice of buffer to use for preparing FIC, and its effect on cellular membrane integrity was evaluated using Lactate Dehydrogenase (LDH) assays (Tox7 Sigma-Aldrich) in 96-well plate format. Cells were plated in densities corresponding to the above determination, at 8.4 x 10^4 cells/well for A549 and H1299, and 21.0 x 10^4 cells/well for Calu-3 cells. A549 cells were passage 20-24, H1299 passage 21-25 and Calu-3 passage 33-35.The three cell lines were incubated with either 0.01M PBS (Phosphate Buffer Saline) or HBSS (Hanks' Balanced Salt Solution) for 2 hours (37°C, 5% CO_2). Each concentration was triplicated. Following the incubation the LDH assay was performed using the manufacturer's recommended method. This involved removing 75.0 µl/well of the cell-conditioned sample solutions and transferring to a fresh, clear 96-well plate. To these solutions 150.0 µl/well LDH reagent was added and the plate incubated at room temperature in the dark for 25 minutes. Immediately after this the absorbance was measured at 492 nm, using a Tecan microplate reader. Plate absorbance was measured at 690 nm and subtracted prior. Blanks were set up that consisted of the same HBSS or PBS solution used for cell-incubations, and LDH added as above, their values then subtracted from the appropriate measurement. Relative LDH release was calculated by setting the absorbance for the untreated cell control (DMEM) as 0%, and the positive control (0.2 % Triton X-100) was assumed to result in total cell lysis and set at 100%.

To determine the effect on metabolic rate of FIC solution in HBSS, we used the MTS ([3-(4,5-dimethylthiazol-2-yl)-5-(3-carboxymethoxyphenyl)-2-(4-sulfophenyl)-2H-tetrazolium) assay (CellTiter 96®, Promega) in 96-well plate format. Cells were seeded as described above for the LDH assay. The three cell lines were incubated with various concentrations (0.001, 0.01, 0.1, 1, 2, 5, 10, 25, 50, 100 mM) of FIC in HBSS for 2 hours (37°C, 5% CO_2). Following incubation, cells were washed once with warm PBS and incubated with 20.0 µl MTS reagent in 100 µl DMEM (without antibiotics, 10% fetal bovine serum (FBS)) *per* well for 2 hours at 37°C and 5% CO_2. Absorbance readings and blank subtractions were taken as described for the LDH assay. Blank subtractions consisted of DMEM with 10% FBS added, without antibiotics. Relative metabolic activity was calculated by setting the absorbance for the untreated cell control (grown in DMEM) as 100%, and the positive control (0.2 % Triton X-100 solution) was assumed to result in total cell lysis and set at 0%.

Electrochemistry on FIC incubated with cells for two hours. A549 cells were passage 17-19, H1299 passage 17-21 and Calu-3 passage 28-29 for these experiments. The three cell lines were seeded at 6.3 x 10^5 cells/well for Calu-3 cells and 2.5 x 10^5 cells/well for A549 and H1299 cells, in a 6 well plate and cultured in DMEM as outlined in the growth study section. The growth medium was removed and each well washed three times with phosphate buffer saline (PBS). Solutions containing only FIC (0.01 mM, 2 ml) was added to the wells and the plates incubated for 2 hours (37°C, 5% CO_2). After the incubation 1ml of the supernatant was removed for electrochemical investigation. All parameters and procedures for electrochemical analysis were followed as outlined above. HBSS buffer was processed as the samples allow for normalisation of the electrochemical data by removing any electrochemical signals arising from the buffer. Bicinchoninic acid assay was carried out as described in **Method S-3**.

pH testing of Hanks' Balanced Salt Solution (HBSS) and 0.01 mM Ferricyanide (FIC), before and after cell incubation. As outlined in **Method S-5** of Supplementary Information.

Inductively coupled plasma mass spectrometry (ICP-MS) to quantitate cellular iron content. As outlined in **Method S-6** of Supplementary Information.

Results and Discussion

It is paramount that we develop new systems to study transplasma electron transport (tPMET) and iron redox chemistry in biological systems. These two areas of study have been implicated within cancer biology[3], and play an instrumental role within iron uptake mechanisms[39,40]. The challenge research currently faces is that eukaryotic cells are notoriously temperamental and subject to extracellular and environmental change. Additionally, when looking at iron redox, FOC is detected as opposed to FIC, where simultaneous detection could be advantageous. This detection of FOC production as opposed to FIC loss is attributable to the poor sensitivity of FIC due to a low extinction coefficient at the 420 nm detection wavelength[7]. In line with this task we have applied electrochemistry to produce an iron quantification system that does not induce cytotoxicity within our cell lines, whilst matching the current world-leader for lower detection limits and improving on this through the simultaneous quantification of two iron redox states.

Calibration curve for iron quantification. Our chosen iron compound for analysis of extracellular reductive capability is FIC with a well-known one electron redox couple[29,32,41]. FIC used in cellular based experiments to report on cellular iron reduction because FIC (Fe^{3+}) can be reduced to FOC (Fe^{2+}) via cellular membrane bound reduction systems[42]. To assess the redox state of iron linear sweep voltammetry was employed[32,33]. The method works by assessing a shift in current values of the current/voltage curve generated within the voltammogram, which indicates a change in the redox state of the iron compound. This is demonstrated in **Figure S-2**, and the corresponding calibration curve is displayed in **Figure S-3**. Cathodic currents (negative values) are indicative of FIC reduction and anodic current (positive current) values represent FOC oxidation. By identifying the position of both steady state anodic and cathodic currents we were therefore able to identify the quantity of FOC and FIC and therefore quantify iron

redox state changes in solution. To allow for this quantification we carried out a characterization study with known concentrations of our redox states, thus producing a calibration curve (**Figure S-3**). The experiment was carried out at the same conditions as all subsequent electrochemical experiments (10 mV s^{-1}, and at 37˚C). This also allowed for the determination of our lower limit of detection (LOD), calculated using the method outline by Armbruster et al[43]. The total iron concentration was kept constant at 0.01 mM whilst only the ratio of oxidized:reduced state was varied. Determination of steady-state was by visual inspection of the first-derivative plot. The potential at which the line intersected the x axis whilst also maintaining a horizontal plateau was selected and the current noted for this point, these current values were then plotted against the known concentrations. The calibration plot generated had a R^2 value of 0.987 for FOC and 0.995 for FIC, as shown in **Figure S-3**. The equations that are used in all later experiments for determination of iron concentration are also displayed in **Figure S-3**, where y is the current and x is the concentration of iron.

The production of FOC by cells has been previously determined using colorimetric methods, most notably by Lawen et al[7]. We calculated our LOD[43] at 0.44 µM for FOC and 0.97 µM for FIC, indicating we are within the same order of magnitude for our system. When calculating our LOD for FOC detection we took our 10:0 FIC:FOC sample (0 mM FOC) to be our blank and 9:1 FIC:FOC (0.001 mM FOC) to be our lowest concentration. We did this as we needed the steady- state anodic current value to use for the calculation. HBSS displays no faradaic current, and therefore it is impossible to test this as a blank.

However, HBSS was tested under the same conditions and subtracted against all electrochemical analysis of iron, therefore normalizing our data to account for the non-faradaic electrochemical contribution from the supporting electrolyte. The LOD calculated using this method provided us with a value in picoamperes, this was then converted into a concentration using our system sensitivities, derived from our equations obtained via **Figure S-3**.

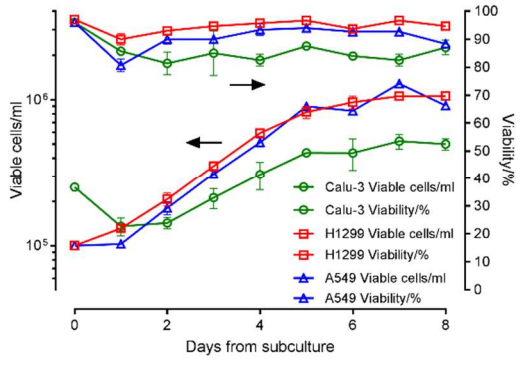

Figure 1. Growth study analysis of Calu-3, A549 and H1229 cells. Calu-3 cells were seeded at 250,000 cell/well, and A549 and H1299 seeded at 100,000 cells/well. Growth profiles show clear lag, exponential and plateau phases. Harvesting times were chosen to be within exponential growth phase. Viability was tested using tryphan blue. N=1, n=3.

The system sensitivity for FOC was 4.67 pA/µM, and for FIC the sensitivity was 4.16 pA/µM. This method was applied for all subsequent iron quantification within additional electrochemical experiments. The same method as above was applied to calculate the LOD for FIC, except cathodic steady-state current values were used. The 95% prediction bands shown in **Figure S-3** show that our data are very precise, with an average 95% prediction band value of +/- 3.71 picoamperes for the linear regression of FOC and +/- 2.20 picoamperes for FIC. This relates to all future values being expected to be within +/- 0.89 µM of the regression line for FOC, and +/- 0.52 µM of the regression line for FIC. This method is also highly precise due to the base subtraction method employed, whereby a buffer-only sample is electrochemically analyzed and is subtracted from the FIC/FOC containing sample, thus removing all chemical noise contribution. If there is no species present within the FIC/FOC sample that passes higher faradaic current than the concentration of FIC/FOC used, then by subtracting the noise in the form of a non-FIC containing blank the analyzed current consist solely of FIC/FOC, and thus vastly reduces the chance of interfering electrochemical species and allowing for highly precise electrochemical analysis.

Growth parameters and toxicity. To begin our cell work we selected three oncogenic cell lines that would allow us to determine whether there was a link between growth rate and their ability to reduce extracellular iron. The chosen cell lines all originate from lung epithelium, and are well characterized within the literature[44,45,46]. It was important to assess the cells growth patterns to ensure cells were harvested within the same growth phase, and to elucidate the cell viability when grown in ideal conditions (FBS-supplemented cell culture medium). This was important because if not within the same growth phase the cells would not be directly comparable, and if the cells viability was compromised we would not be analyzing a repeatable system. Therefore we performed a growth study (**Figure 1**). Assessment of growth rate was done using a Tecan plate reader with cell counting and viability functions and needed optimizing which is discussed in SI **Method S-4**. As can be seen from **Figure 1**, our growth curves show a defined lag, exponential and plateau phases. Harvesting time was chosen at three days for H1299 cells and A549 cells, and four days for Calu-3 cells. These times were chosen as all cell lines would then be in the same phase of growth, but also the cell number for Calu-3 cells would be more comparable to A549 and H1299 cells after four days. We needed to determine the doubling time of the cells to have a quantifiable measure of the proliferative rate of the cells (also tell you about the cell cycle is effected by toxicity). Doubling time was determined by taking the same portion of the exponential phase, 200,000 to 400,000 cells/ml, and calculating the time taken in days to achieve this doubling. H1299 cells had the quickest doubling time at 0.816 days, followed by A549 cells at 1.123 days, and finally Calu-3 cells at 3.804 days. The doubling times achieved mimic the literature for A549 and H1299 cells[47], and

to the best of our knowledge a value for Calu-3 doubling time could not be found. The range of cell

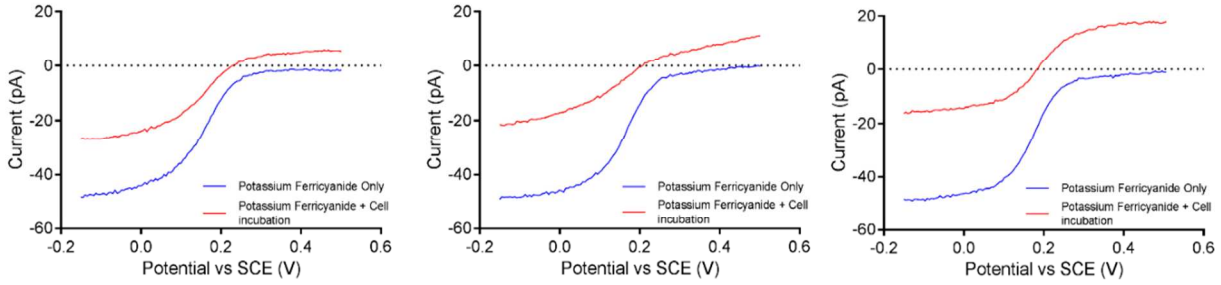

Figure 2. Examples of linear sweep voltammogram obtained for each cell line. Cell were exposed to solutions of 0.01 potassium ferricyanide for 2 hours prior to supernatants being taken for electrochemical analysis. Calu-3 (left), H1299 (middle), A549 (right). Hank's Balanced Salt Solution (HBSS) buffer with 0.01 mM potassium ferricyanide in the absence (blue) and presence (red) of cells. Scan rate, 10 $mV.s^{-1}$. N=3, n=3.

types we have chosen therefore allows us to compare A549 and H1299 cells which have a similar doubling rate of 0.816 and 1.123, with the less proliferative cell line Calu-3. It was important that we checked cell viability to ensure we were not providing a stressful environment to the cells, which in turn can cause changes in metabolism[48]. Cell viability in ideal conditions, as demonstrated on the right-hand axis of **Figure 1**, demonstrates the cell lines are in a favorable environment prior to treatment with iron.

Having characterized the growth system for this experiment the choice of buffer to be used as our supporting electrolyte, as well as any cytotoxicity in response to FIC/FOC, was analyzed. The employment of a highly sensitive electrochemical system meant the presence of electrochemically active species in the supporting electrolyte had to be considered, as they may have contributed to the signal that was collected. Additionally, the supporting electrolyte had to be the correct osmolality to ensure cytolysis did not occur, and that the cells did not undergo undue stress. Two commonly used salt-based cell culture buffers were tested – PBS and HBSS. The main differences between these buffers are their salt components, in addition to the presence of magnesium ions, calcium ions, and D-glucose within HBSS.

PBS was chosen as it is a more minimal salt buffer in comparison to HBSS, thus there would be little scope for it to electrochemically interfere with our analytical signal. HBSS was chosen as, although it has more components, the added magnesium and calcium are important for cell adhesion, and the D-glucose present provided a substitute for serum ensuring the cells had an energy source. An LDH assay and the MTS assay was performed with cells exposed to the different electrolyte. The LDH assay measures cell membrane integrity and so gave us an indication of whether the membrane was perturbed, which is indicative of cell death. Iron interferes with the LDH assay so only buffer was assessed here. The MTS assay measures metabolic activity, and therefore is indicative of sub-lethal toxicity. Iron cytotoxicity was assayed in this way, after a suitable buffer was chosen. This allowed us to indirectly assess irons effect upon membrane integrity as the MTS assay was carried out with iron in solution with the preferred buffer.

LDH assay data is shown in **Figure S-6A**. It demonstrates that HBSS is the preferred buffer, relative to PBS, although the LDH release is relatively low in both cases. The MTS assay data on toxicity of FIC is displayed in Figure S-6B, and demonstrates FIC in HBSS does not become cytotoxic over two hours until ~10 mM concentration. This meant that our chosen concentration of 0.01 mM was suitable. The LDH and MTS assays data are discussed in further detail in the Figure S-6 section of the Supplementary Information.

Electrochemical analysis of cell-incubated samples. The cell culture conditions and electrochemical assay that we developed and characterised were used to assess the cells ability to reduce FIC to FOC. Solutions of FIC were first analyzed by generating a linear sweep voltammogram (LSV) of FIC solutions only **(Figure 2)**. The solutions of FIC were incubated with the cells for two hours at 37°C and 5% CO_2, before LSVs were generated of the supernatants of the incubated FIC samples **(Figure 2)**. FIC only samples **(Figure 2, blue)** produced only cathodic (reductive) currents, with the anodic steady state plateauing at 0 pA, thus indicating the absence of FOC. Upon incubation with each cell line an upward shift in the current measurements was observed **(Figure 2, red)**, indicating a shift of redox states to both FOC and FIC. When incubated with the cells we can deduce that FIC is reduced to FOC, and thus when we scan across our potential range both oxidation and reduction occurs as both redox states undergo electron transfer. It can clearly be observed visually that Calu-3 cells (left) reduce less iron than H1299 (middle), and H1299 cells in turn reduce less than A549 cells (right). It is also apparent that there is a slight change in the shape and half-wave potentials of the voltammograms. We suggest that this may be due to minor changes in the pH of the solutions and potential pH

discrepancies between HBSS and FIC after cell incubation. The pH data is presented in Figure S-7 and discussed therein. It is well established that pH can affect the half-wave potential of such electrochemical reactions as we have previously reported [32].

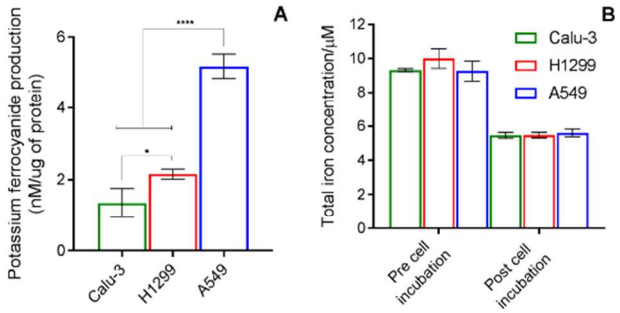

Figure 3. Electrochemical analysis of cellular reduced 0.01 mM potassium ferricyanide in Hank's Balanced Salt Solution (HBSS) buffer. **(A)** Concentration of potassium ferricyanide produced, normalized by protein quantification. Statistical analysis was carried out using a one-way ANOVA with Tukey's multiple comparisons test at P = 0.0453 for Calu-3 vs H1299, and P = 0.0001 for all other comparisons. N=3, n=3. **(B)** Total iron concentration before and after cell incubation. Pre cell incubation samples are significant to P = 0.0001 for all cell types, compared to post cell incubation samples. This was determined by two-way ANOVA with Sidak's multiple comparisons test. SEM error bars shown N=3, n=3. Cell appear to be viable in optimal conditions, and undergo stress when transferred into an alternative medium.

Quantification of iron reduction and comparison between cell types. Quantification of the iron reduction was calculated using steady states from both FIC only **(Figure 2, blue)** and FIC/FOC after cell incubation **(Figure 2, red)** samples from **Figure 2**. Determination of steady states and subsequent iron quantification calculations employed the same method outlined for our calibration plot. The steady states for these calculations were determined using the data presented in **Figure 2 (blue and red)**, once again using the method outlined for our calibration plot. **Figure 3A** shows the amount of FOC produced by the cell lines, which has been normalised for the amount of protein present in each well plate, thus allowing direct comparison between cell lines. The amount of FOC produced in nM per ug of protein was 1.25, 2.18 and 5.19 for Calu-3, H1299 and A549 cells respectively. The significance of these results was determined using an one-way ANOVA with Tukey's multiple comparison test, which showed significance between Calu-3 and H1299 reduction of p = 0.0084 and A549 to all other cell lines of p = 0.0001. The robustness of our system in analysing this reduction is also demonstrated with our low coefficients of variation (%CVs) internally between cell samples, at 15.80, 7.41 and 6.58% for Calu-3, H1299 and A549 cells respectively. The importance of these results is indicated when taking data from our doubling times data, mitochondrial metabolic rates, and **Figure 3A**. We can observe that there is no link between the doubling time, and therefore cell cycle differences between the cells, and the amount of FOC produced. In addition, there is no link between mitochondrial metabolic rate and FOC production. Although FOC production is increased when comparing our least proliferative cell line (Calu-3) to our other two (A549 and H1299), we would expect H1299 to have a marginally higher reductive power in relation to A549 cells, or at least to have a similar reductive power when comparing to proliferation, but A549 cells reduce 3.01 nM/ug of protein more FIC than H1299 cells. Our rationale behind a possible link with mitochondrial metabolic rate and therate of tPMET activity was that higher metabolic rate cells would have a faster turnover of reversible redox couples, and as such have more capability to reduce iron via tPMET. This was not the case, where Calu-3 cells with the highest metabolic rate reduce the least iron (and therefore have the lowest tPMET activity) whilst H1299 with the lowest mitochondrial metabolic rate have a higher tPMET activity. This highlights how important it is to study tPMET systems in biology, as there is evidently much to be understood about how the underlying biology and biochemistry of the cells affects these transport mechanisms. It has been suggested[18] that trans plasma membrane electron transport (tPMET) can occur via two mechanisms: either through membrane-bound oxidoreductase activity, or through a shuttle-based system exporting reducing equivalents. We hypothesise that a mixture of these systems is in play here, and in subsequent research will hope to elucidate the exact mechanisms of the reduction we have detected here, in addition linking the biological causes of these cell lines have differing reductive capabilities.

Figure 3B shows the quantification of total iron concentration. We observe a reduction in total iron concentration across all cell lines after incubation with the cells. This is significant at p = 0.001 for all cell lines, as assessed by two-way ANOVA with Sidak's multiple comparison test. It was important to demonstrate that FIC was not entering the cell as the goal of these investigations was to study tPMET and not iron reduction via internal electron transfer systems inside of the cell. A landmark paper by Keilin et al [49] showed that FIC does not cross the plasma membrane. However we wished to confirm this and therefore performed ICP-MS to quantitate cellular iron. With the premise being if FIC was entering the cell we would see an increase in cellular iron content when cells were incubated with solutions of FIC versus in its absence.

Our data represented in **Figure S-8** corroborates with Keilin et al, and proves for our system that the iron content of the cell is not affected by incubation with FIC. This in turn means that neither FIC nor FOC are entering into, or adhering onto the surface of the cells. Iron content values *per* cell for HBSS incubated samples were 0.14, 0.12 and 0.13 pg for Calu-3, H1299 and A549 cells respectively, and 0.15, 0.12 and 0.10 pg respectively for FIC incubated samples. Two-

way ANOVA with Sidak's multiple comparison test showed no significant different with between HBSS or FIC incubated samples, and no significant difference between cell lines. The iron content of the cells appears to be in line with the literature when normalised for cell number, Mathiasen et al [50] present iron levels for mesenchymal stem cells of 0.48 pg/cell, Mojic et al [51] present values of 0.3 pg/cell for prostate cancer cell lines LNCaP and PC3, and although an untreated sample is not shown, Kumar et al [52] present A549 cells as having ~2.8 pg of iron/cell when incubated with superparamagnetic iron oxide nanoparticles, indicating that pictograms are in line with expected values. Another important point to note is that our stability data indicates this reduction in total iron concentration cannot be from instability and subsequent deterioration of the redox couple under variable conditions. In addition to this we tested whether the electrode would be fouled by using cell-incubated material to ensure that this was not the cause of total iron reduction (SI Figure S-4). We performed the analysis on cells in PBS as the membrane integrity for PBS incubated cells was lower (LDH assay, SI Figure S6) and thus there would be more potential for electrode fouling by released components. We found there to be no evidence of electrode fouling, as demonstrated by paired t-test of a 0.01 mM FIC solution electrochemically analysed before and after the microelectrode has been used with a cell-incubated sample, at $p = 0.1406$. In light of our findings, we would therefore tentatively suggest that FIC and/or FOC is interacting electrostatically with a cell-effluxed molecule, thus resulting in a 'loss' of FIC and/or FOC from the supernatant.

Interestingly, this detection of a change in total iron concentration highlights one of the major advantages of using an electrochemical method to quantitate FOC production. Improving on the colorimetric methods of Lane et al, and Avron and Shavrit, our system allows for the quantification of both the oxidised and reduced states, as opposed to only the reduced state. This advancement is already having highly relevant and impactful ramifications, as it has flagged interesting findings in our system that would not have been detected if we had employed the colorimetric method. Combined with matching Lane et al as the current world-leader in detection limit for FOC, this provides a very robust system to analyze cellular-induced FOC production. Additionally, another interesting advantage is the lack of requirement for addition of acid to the sample.

Conclusion

Here we have demonstrated a novel application for analytical electrochemistry by quantitating cellular iron reduction in oncogenic eukaryotes, and by doing so have created a highly sensitive system that can be used to detect quantities of both FIC and FOC simultaneously. The technique contends with the current world leaders for detection limits of FOC, and provides a detection limit for FIC also that is within the same order of magnitude. We have used linear sweep voltammetry to assess the iron reduction capability of three lung cancer cell lines, and link this to the proliferative rates and mitochondrial metabolic rates of the cell lines in question. Furthermore, the reproducibility of our cell work with relatively low variability in the spread of the data for a biological system, once again demonstrating the robustness of this model for investigation. We have identified differences in iron reduction capability, showing that a higher proliferative rate or metabolic rate does not necessarily result in a higher reductive capability, highlighting a deficiency in the biological knowledge of these systems. This work will be highly relevant and have high impact across a diverse set of fields, driving forward multidisciplinary research especially in relation to tPMET systems[53] and their presence in oncogenic cell lines[3]. It also provides an insight into the biology of our studied cell lines, which are commonly used as lung epithelium models. Moreover the developed assay offers a generic technique to study tPMET in any cells.

ASSOCIATED CONTENT

Supporting Information

The Supporting Information is available free of charge on the ACS Publications website.
Stability of FIC in cell culture conditions. Simultaneous quantification of iron redox states for the stability of FIC and FOC at 37ºC and 5% CO2. Bicinchoninic acid assay. Cell mycoplasma testing. Iron redox state concentration calibration study. Calibration curve for potassium ferrocyanide (FOC) and potassium ferricyanide (FIC). Assessment of growth rate using a Tecan plate reader with cell counting and viability functions. Growth rate study for Calu-3 cells. Inductively coupled plasma mass spectrometry (ICP-MS). (PDF)

AUTHOR INFORMATION

Corresponding Author

*Email: Frankie.Rawson@nottingham.ac.uk

Author Contributions

All authors have given approval to the final version of the manuscript.

Notes

The authors declare no competing financial interest.

ACKNOWLEDGMENT

The authors thank the Engineering and Physical Sciences Research Council (EPSRC; EP/L01646X), The University of Nottingham CDT in Advanced Therapeutics and Nanomedicines, and Boots UK Ltd for financial Support. We would also like to thank the Division of Agriculture & Environmental Sciences School of Biosciences (Sutton Bonington Campus Nr Loughborough, LE12 5RD) for their help with ICP-MS samples analysis.

REFERENCES

(1) Rawson, F. J.; Garrett, D. J.; Leech, D.; Downard, A. J.; Baronian, K. H. R. *Biosens. Bioelectron.* **2011**, *26* (5), 2383–2389.
(2) Haslett, N. D.; Rawson, F. J.; Barriëre, F.; Kunze, G.; Pasco,

N.; Gooneratne, R.; Baronian, K. H. R. *Biosens. Bioelectron.* **2011**, *26* (9), 3742–3747.

(3) Herst, P. M.; Tan, A. S.; Scarlett, D.-J. G.; Berridge, M. V. *Biochim. Biophys. Acta* **2004**, *1656* (2–3), 79–87.

(4) Lane, D.; Bae, D.-H.; Merlot, A.; Sahni, S.; Richardson, D. *Nutrients* **2015**, *7* (4), 2274–2296.

(5) Ghio, A. J.; Turi, J. L.; Yang, F.; Garrick, L. M.; Garrick, M. D. *Biol. Res.* **2006**, *39* (1), 67–77.

(6) Ghio, A. J. *Biochim. Biophys. Acta - Gen. Subj.* **2009**, *1790* (7), 731–739.

(7) Lane, D. J. R.; Lawen, A. *Anal. Biochem.* **2008**, *373* (2), 287–295.

(8) Kostas Pantopoulos, Suheel Kumar Porwal, Alan Tartakoff, and L. D. *Mechanisms of mammalian iron homeostasis*; 2012; Vol. 29.

(9) Lieu, P. T.; Heiskala, M.; Peterson, P. a.; Yang, Y. *Mol. Aspects Med.* **2001**, *22* (1–2), 1–87.

(10) Kamga, C.; Krishnamurthy, S.; Shiva, S. *Nitric Oxide - Biol. Chem.* **2012**, *26* (4), 251–258.

(11) Hentze, M. W.; Muckenthaler, M. U.; Andrews, N. C. *Trends Biochem. Sci.* **2005**, *30* (3), 285–297.

(12) Lane, D. J. R.; Lawen, A. *Free Radic. Biol. Med.* **2009**, *47* (5), 485–495.

(13) Medina, M. Á.; Castillo-Olivares, A. Del; De Castro, I. N. *BioEssays* **1997**, *19* (11), 977–984.

(14) Wolvetang, E. J.; Larm, J. A.; Moutsoulas, P.; Lawen, A. *Cell Growth Differ.* **1996**, *7* (10), 1315–1325.

(15) Lawen, A.; Baker, M. A.; Malik, S. *Protoplasma* **1998**, *205* (1), 10–20.

(16) May, J. M. *FASEB J.* **1999**, *13* (9), 995–1006.

(17) McKie, A. T.; Barrow, D.; Latunde-Dada, G. O.; Rolfs, A.; Sager, G.; Mudaly, E.; Mudaly, M.; Richardson, C.; Barlow, D.; Bomford, A.; Peters, T. J.; Raja, K. B.; Shirali, S.; Hediger, M. A.; Farzaneh, F.; Simpson, R. J. *Science* **2001**, *291* (5509), 1755–1759.

(18) Lane, D. J. R.; Lawen, A. *BioFactors* **2009**, *34* (3), 191–200.

(19) Lane, D. J. R.; Lawen, A. *Free Radic. Biol. Med.* **2009**, *47* (5), 485–495.

(20) Su, D.; May, J. M.; Koury, M. J.; Asard, H. *J. Biol. Chem.* **2006**, *281* (52), 39852–39859.

(21) Turi, J. L.; Wang, X.; McKie, A. T.; Nozik-Grayck, E.; Mamo, L. B.; Crissman, K.; Piantadosi, C. A.; Ghio, A. J. *Am J Physiol Lung Cell Mol Physiol* **2006**, *291* (2), L272-80.

(22) Kovar, J.; Neubauerova, J.; Cimburova, M.; Truksa, J. *Blood Cells. Mol. Dis.* **2006**, *37*, 95–99.

(23) Loke, S.; Siddiqi, N. J.; Alhomida, A. S.; Kim, H.; Ong, W. *Neuroscience* **2013**, *245*, 179–190.

(24) Balusikova, K.; Neubauerova, J.; Dostalikova-Cimburova, M.; Horak, J.; Kovar, J. *Mol. Cell. Biochem.* **2009**, *321* (1), 123–133.

(25) Anderson, G. J. *Journal of Gastroenterology and Hepatology (Australia)*. 1999, pp 105–108.

(26) Brissot, P.; Ropert, M.; Le Lan, C.; Loréal, O. *Biochim. Biophys. Acta - Gen. Subj.* **2012**, *1820* (3), 403–410.

(27) Warburg, O. ed. *J. Am. Med. Assoc.* **1931**, *96*, 1982–2309.

(28) Herst, P. M.; Berridge, M. V. *Biochim. Biophys. Acta - Bioenerg.* **2007**, *1767* (2), 170–177.

(29) Oakhill, J. S.; Marritt, S. J.; Gareta, E. G.; Cammack, R.; McKie, A. T. *Biochim. Biophys. Acta - Bioenerg.* **2008**, *1777* (3), 260–268.

(30) Mackenzie, B.; Ujwal, M. L.; Chang, M.-H. H.; Romero, M. F.; Hediger, M. a. *Pflugers Arch. Eur. J. Physiol.* **2006**, *451* (4), 544–558.

(31) Mackenzie, B.; Takanaga, H.; Hubert, N.; Rolfs, A.; Hediger, M. a. *Biochem. J.* **2007**, *403* (1), 59–69.

(32) Rawson, F. J.; Downard, A. J.; Baronian, K. H. *Sci. Rep.* **2014**, *4*, 5216.

(33) Baronian, K.; Downard, A.; Lowen, R.; Pasco, N. *Appl. Microbiol. Biotechnol.* **2003**, *60* (1–2), 108–113.

(34) McDowall, J. S.; Ntai, I.; Honeychurch, K. C.; Hart, J. P.; Colin, P.; Schneider, B. L.; Brown, D. R. *Mol. Cell. Neurosci.* **2017**, *85* (Supplement C), 1–11.

(35) Herst, P. M.; Berridge, M. V. *Biochim. Biophys. Acta - Bioenerg.* **2007**, *1767* (2), 170–177.

(36) Berridge, M. V.; Herst, P. M.; Tan, A. S. *Mitochondrion* **2010**, *10* (6), 584–588.

(37) Scarlett, D. J.; Herst, P.; Tan, a; Prata, C.; Berridge, M. *Biofactors* **2004**, *20* (4), 199–206.

(38) Avron, M.; Shavit, N. *Anal. Biochem.* **1963**, *6* (6), 549–554.

(39) Lawen, A.; Lane, D. J. R. *Antioxid. Redox Signal.* **2013**, *18* (18).

(40) Ganz, T. *Physiol. Rev.* **2013**, *93* (4), 1721–1741.

(41) Kissinger, P. T.; Heineman, W. R. *J. Chem. Educ.* **1983**, *60* (9), 702.

(42) Sun, I. L.; Crane, F. L.; Grebing, C.; Löw, H. *J. Bioenerg. Biomembr.* **1984**, *16* (5), 583–595.

(43) Armbruster, D. A.; Pry, T. *Clin. Biochem. Rev.* **2008**, *29 Suppl 1* (August), S49-52.

(44) Blanco, R.; Iwakawa, R.; Tang, M.; Kohno, T.; Angulo, B.; Pio, R.; Montuenga, L. M.; Minna, J. D.; Yokota, J.; Sanchez-, M. *Hum. Mutat.* **2010**, *30* (8), 1199–1206.

(45) Lieber, M.; Todaro, G.; Smith, B.; Szakal, A.; Nelson-Rees, W. *Int. J. Cancer* **1976**, *17* (1), 62–70.

(46) Shen, B. Q.; Finkbeiner, W. E.; Wine, J. J.; Mrsny, R. J.; Widdicombe, J. H. *Am. J. Physiol.* **1994**, *266* (5 Pt 1), L493-501.

(47) Chan, K.-S.; Koh, C.-G.; Li, H.-Y. *Cell Death Dis.* **2012**, *3*, e411.

(48) Cairns, R. A.; Harris, I. S.; Mak, T. W. *Nat. Rev. Cancer* **2011**, *11* (2), 85–95.

(49) Keilin, F. R. S.; Hartree, E. . *Nature* **1946**, *157*, 210.

(50) Mathiasen, A. B.; Hansen, L.; Friis, T.; Thomsen, C.; Bhakoo, K.; Kastrup, J. *Stem Cells Int.* **2013**, *2013*.

(51) Mojić, M.; Bogdanović Pristov, J.; Maksimović-Ivanić, D.; Jones, D. R.; Stanić, M.; Mijatović, S.; Spasojević, I. *Sci. Rep.* **2014**, *4*, 5955.

(52) Kumar, M.; Singh, G.; Arora, V.; Mewar, S.; Sharma, U.; Jagannathan, N. R.; Sapra, S.; Dinda, A. K.; Kharbanda, S.; Singh, H. *Int. J. Nanomedicine* **2012**, *7* (September), 3503–3516.

(53) Ly, J. D.; Lawen, A. *Redox Rep.* **2003**, *8* (1), 3–21.

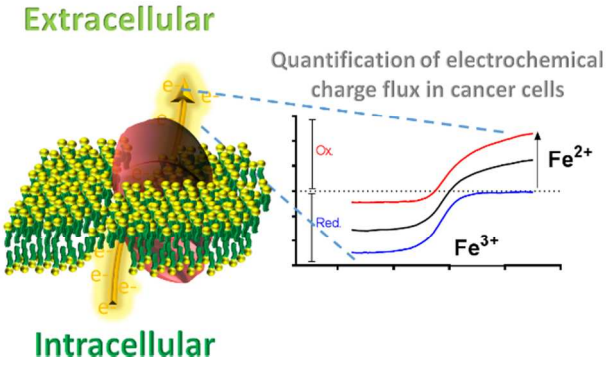
Extracellular
Quantification of electrochemical charge flux in cancer cells
Ox
Red
Fe^{2+}
Fe^{3+}
Intracellular

1
2